Rhus trilobata Nutt. (Anacardiaceae)

Subjects: Plant Sciences

Contributor: Luis Varela-Rodríguez

Rhus trilobata (RHTR) is a medicinal plant with cytotoxic activity in different cancer cell lines. However, the active compounds in this plant against ovarian cancer are unknown. In this study, we aimed to evaluate the antineoplastic activity of RHTR and identify its active metabolites against ovarian cancer. The aqueous extract (AE) and an active fraction (AF02) purified on C18-cartridges/ethyl acetate decreased the viability of SKOV-3 cells at 50 and 38 µg/mL, respectively, compared with CHO-K1 (> 50 µg/mL) in MTT assays and generated changes in the cell morphology with apoptosis induction in Hemacolor® and TUNEL assays ($p \leq 0.05$, ANOVA). The metabolite profile of AF02 showed a higher abundance of flavonoid and lipid compounds compared with AE by UPLC-MS. Gallic acid and myricetin were the most active compounds in RHTR against SKOV-3 cells at 50 and 166 µg/mL, respectively ($p \leq 0.05$, ANOVA). Antineoplastic studies in *Nu/Nu* female mice with subcutaneous SKOV-3 cells xenotransplant revealed that 200 mg/kg/i.p. of AE and AF02 inhibited ovarian tumor lesions from 37.6% to 49% after 28 days ($p \leq 0.05$, ANOVA). In conclusion, RHTR has antineoplastic activity against ovarian cancer through a cytostatic effect related to gallic acid and myricetin. Therefore, RHTR could be a complementary treatment for this pathology.

Keywords: antineoplastic activity ; gallic acid ; myricetin ; ovarian cancer ; Rhus trilobata

1. Introduction

Ovarian cancer is the sixth most frequent tumor in women and the fourth cause of death in Mexico due to gynecological tumors [1]. Ovarian tumors can be primary or metastatic and are classified based on their origin as epithelial, germinal, or stromal of the sexual cord tumors [2]. Epithelial tumors are the most common type of ovarian neoplasm; among them, the serous subtype usually appears more frequently [2]. Surgical resection is the principal treatment for this disease, followed by antitumoral chemotherapy with cytotoxic or cytostatic drugs [1][3]. However, the surgent of resistance in neoplastic tissue limits ovarian cancer chemotherapy's success [3], making it necessary to search for alternative treatments or new therapeutic agents for this disease. Plants used for alternative medicine represent an option in the search for active compounds for cancer treatment. Recent work with *Rhus trilobata* Nutt. (RHTR) demonstrated the presence of antineoplastic agents that could be new therapeutic candidates for the treatment of ovarian cancer that afflicts the female population in Mexico and around the world [4].

In Mexico, RHTR (*Anacardiaceae* family) is used for the treatment of gastrointestinal diseases and cancer. RHTR is known by the common name of *aciditos* or *agritos* due to the characteristic flavor of its fruit [4]. Previous studies by Abbott et al. (1966) demonstrated the antineoplastic activity of RHTR in Syrian hamsters xenotransplanted with duodenum adenocarcinoma. Animals were treated with extracts of leaves (100 mg/kg/i.p.) or fruits (400 mg/kg/i.p.) for seven days; tumoral lesions decreased 33% with both extracts in comparison with control conditions [5]. Subsequently, Pettit et al. (1974) isolated gallic acid (Ga) from RHTR leaves with column chromatography (Sephadex LH-20) and determined its biological activity; Ga decreased KB cell viability (IC_{50}: 3.1 µg/mL). The authors concluded that the medicinal properties of RHTR correspond to this compound [6]. Studies conducted by our research group revealed that the aqueous extract (AE) of RHTR stems contains quinic acid, myricetin (Myr), Ga, 1,2,3,4,6-pentakis-*O*-gallioyl-*β*-D-glucose (*β*-PGG), quercetin, obtusaquinol, fisetin, margaric acid, and amentoflavone by UPLC-MS^E, which are compounds with biological activity already demonstrated by other studies [4]. Additionally, AE-RHTR presented a selective activity against CACO-2 cells (IC_{50}: 5 µg/mL), and low toxicity (LD_{50}: 1141.5 mg/kg) [4]. Thus, the biological activity observed in RHTR may be related to compounds such as phenolic acids or flavonoids and the synergic effects between both molecule types.

2. Biological Activity of AE-RHTR and Fractions in Cell Lines

The AE and fractions from RHTR presented biological activity in SKOV-3 cells at 50 µg/mL (**Figure 1**A). In comparison, the concentration required to affect the viability of CHO-K1 cells was greater than 50 µg/mL (**Figure 1**B), demonstrating a selective effect. AE and AF02 were most active against SKOV-3 cells at 50 and 38 µg/mL, respectively, compared with 1×

PBS (vehicle group) ($p < 0.05$, Dunnett). However, AE and AF02 were found to only have a 24 h limited inhibitory effect on SKOV-3 cell proliferation (**Figure 1**C). Additionally, SKOV-3 cells treated with AE and AF02 had a similar morphology to the vehicle group but with a considerable increase in cytoplasmic vesicles and an absence of cellular mitosis, which suggest a quiescent effect in both treatments (**Figure 1**D). The apoptosis assays mainly demonstrated increased caspase-3/7 activity and nuclear DNA-fragmentation in cells treated with AE (8.47% ± 0.9%), AF02 (14.01% ± 3.7%), and paclitaxel (46.42% ± 5.0%) at 24 h in comparison with the vehicle group (2.47% ± 0.4%) ($p < 0.05$, ANOVA; **Figure 1**D,E). Necrotic events were present during treatments with both samples at 72 h (**Figure 1**E), possibly related to stages of late apoptosis and not with true necrosis, which can promote inflammatory processes; however, additional studies are necessary to corroborate this finding. These results resemble those obtained with CACO-2 cells, where cell cycle arrest in G_1 and the appearance of a G_1 subpopulation related to apoptosis were observed. In contrast, in BEAS-2B cells, increasing the concentration up to 800 µg/mL was necessary to observe a similar effect [4]. Therefore, AE and AF02 were selected to evaluate their antineoplastic activity.

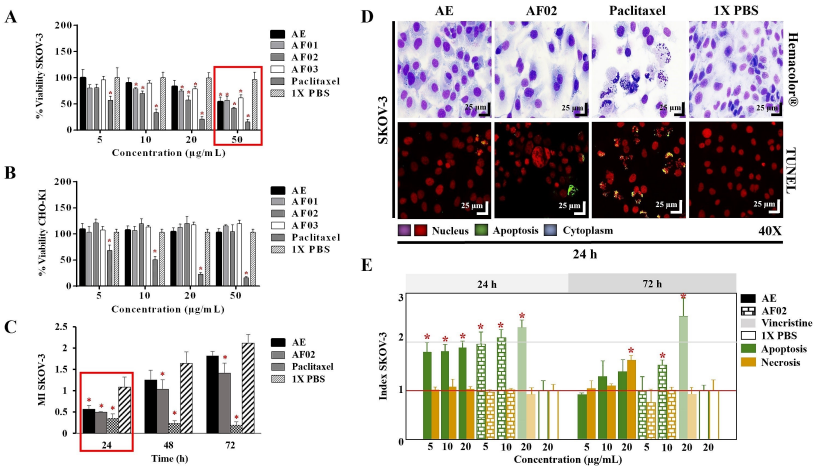

Figure 1. Biological activity of RHTR in ovarian cancer. The IC_{50} of AE and fractions in SKOV-3 (**A**) and CHO-K1 (**B**) cell lines were obtained with dose–response viability curves at 24 h by MTT assay. The antiproliferative (**C**), cytotoxic, and apoptotic (**E**) activities of AE and AF02 were determined in SKOV-3 cells by an ApoTox-Glo™ Triplex Assay. The morphological changes with Hemacolor® rapid staining and TUNEL were observed at 24 h of treatment with AE (50 µg/mL) and AF02 (38 µg/mL), respectively (**D**). The results show the mean ± SD of three biological replicates ($n = 3$, in triplicates). * $p \leq 0.05$ vs. the control group without treatment (1× PBS) (ANOVA). Paclitaxel or vincristine was used as the positive control. MI, mitotic index (*MI = Abs sample/Abs control*); RHTR, *Rhus trilobata*; AE, aqueous extract; AF, aqueous fraction (numbers indicate the fraction obtained after fractionation on the solid phase with solvents, as described in the Methodology section).

3. Antineoplastic Activity of RHTR in Mice Xenotransplanted with SKOV-3 Cells

After 24 h of treatment, the rodents showed no behavioral changes. Additionally, the analyses of their bodyweight showed that the group treated with AE experienced a 9.5% decrease, but a 3.7% increase in the group with AF02. However, these changes were not significant compared to the control group treated with 1× PBS vehicle ($p > 0.05$, Dunnett; **Figure 2**A). At the end of treatments, mice were euthanized for tumor lesions recovery and to perform a macroscopic analysis of the developed lesions (**Figure 2**C). Similar characteristics in all tumors were present in the treated groups with an ovoid or smooth-surfaced morphology and the presence of vascularity (**Figure 2**C). However, minor differences in the color of tumors were found: pink for AE and whitish for AF02; groups treated with carboplatin and vehicle presented a yellow tumor with a nodular surface (**Figure 2**C). Analysis of tumoral weight showed that greater masses were found in the vehicle group, followed by AE, AF02, and carboplatin ($p > 0.05$, Tukey; **Table 1**). These results correlate with the tumor volume of lesions present in rodents along with the treatment time (**Figure 2**B). The inhibition percentage in tumoral growth with AE, AF02, and carboplatin was 37.6%, 49%, and 74.5%, respectively, compared with the control group for 14 and 28 days of treatment ($p \leq 0.05$, Dunnett; **Figure 2**B,C). These findings demonstrate changes in the disease evolution directly related to the treatments used in the study. Similarly, these results agree with those obtained in tumoral length (**Table 1**), which demonstrated a cytostatic effect of the treatments.

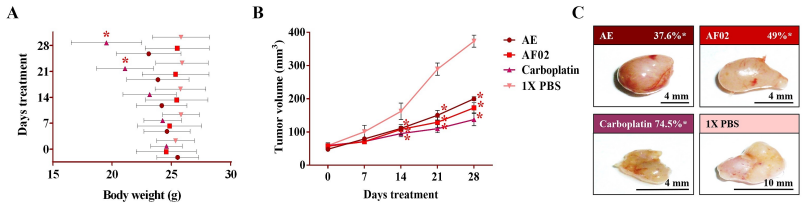

Figure 2. Antineoplastic activity of AE and AF02 from RHTR in ovarian cancer. The bodyweight of rodents was monitored with an electronic bascule for 28 days (**A**). The tumor volume was determined with a Vernier caliper in mice treated with AE and AF02 at 200 mg/kg/i.p./day (Tumoral volume = [Larger diameter × (Shorter diameter)^2]/2) (**B**). Morphological changes in tumor lesions were analyzed at the end of treatments, and the percent inhibition was calculated (**C**). Results show the mean ± SD of two biological replicates (n = 5). * $p \leq 0.05$ vs. the control group without treatment (1× PBS) (ANOVA). The positive control was carboplatin (50 mg/kg/i.p./3 alternating days per week in mice). RHTR, *Rhus trilobata*; AE, aqueous extract; AF02, aqueous fraction-02 (active fraction obtained with ethyl acetate).

Table 1. Morphological characteristics of ovarian tumor lesions treated with RHTR.

Treatments	AE	AF02	Carboplatin	1× PBS
Weight (g)	**0.24 ± 0.09 ***	**0.19 ± 0.10 ***	**0.14 ± 0.06 ***	**0.34 ± 0.09**
Larger diameter (mm)	**9.07 ± 0.25 ***	**7.40 ± 0.95 ***	**3.70 ± 0.26 ***	**14.53 ± 2.4**
Tumor volume (mm^3)	**201.4 ± 11.6 ***	**172.7 ± 15.3 ***	**137.3 ± 18.6 ***	**373.3 ± 18.1**
Attenuation coefficient (HU)	**47 ± 2.16**	**48.8 ± 0.83**	**48.7 ± 0.95**	**47 ± 2.1**
Vascularity	**+**	**+**	**+**	**+++**
Fibrosis	**+**	**+**	**+**	**+**
Morphology	**Cystic**	**Cystic**	**Solid**	**Cystic**

Results show the mean ± SD of two biological replicates (n = 5). * $p \leq 0.05$ vs. control values treated with 1× PBS vehicle (ANOVA). The positive control was carboplatin (50 mg/kg/i.p./3 alternating days per week in mice). HU, Hounsfield unit; +, present; +++, abundant. RHTR, *Rhus trilobata*; AE, aqueous extract; AF02, aqueous fraction-02 (active fraction).

3.1. Imaging and Histopathological Studies of Tumor Lesions

Images by NMR showed ovoid tumors located in the subcutaneous tissue, with attenuation units related to soft tissues (≈50 HU; **Table 1**). Treatments with AE and AF02 induced regular edges in tumoral lesions, whereas groups treated with carboplatin and vehicle were mainly lobulated edges (**Figure 3**A). Additionally, the necrosis percentage was higher in mice treated with vehicle (35.16%), whereas those treated with AE, AF02, and carboplatin were 30.68%, 20.54%, and 5.19%, respectively (**Figure 3**A). Images by USG corroborated the presence of subcutaneous ovoid tumors, with partially defined edges and heterogeneous content (hyperechoic areas with diffuse distribution concerning fibrosis) in the different groups (**Figure 3**B). Vascularity presence was observed in all tumors (seen as red and blue color); however, the highest vascularity was found in mice treated with vehicle compared with AE, whereas the lower vascularity was observed in those animals treated with AF02 or carboplatin (**Figure 3**B). The histological analysis of cystic lesions located in the reticular dermis of rodents revealed a stroma/parenchyma of mixed composition and without residual organ (**Figure 3**C). The abundant presence of loose fibrous tissue was observed in all tumors with a predominance of comedo-type necrosis for the vehicle (25%), decreasing by AE and AF02 treatment (10%), or basaloid-type histological pattern after carboplatin (**Figure 3**C, H&E). Additionally, the adjacent stroma in tumors presented retraction artifacts (cracks) and signs of acute/moderate chronic inflammation by variable cellular infiltrate (**Figure 3**C, H&E). Other characteristics observed in all tumors were the proliferation of basaloid cells (basement membrane cells-like) organized in a solid pattern that grew to push the stroma, as well as palisade cells on the tumor periphery with a radial orientation at superior parallel axes (**Figure 3**C, H&E and TOB). Similarly, most cells presented mixed nuclei (small and hyperchromatic) with vesicular chromatin and a poorly defined wide eosinophilic cytoplasm (**Figure 3**C, H&E). RHTR treatments induced atypical mitosis and apoptosis in comparison with the control group (**Figure 3**C, TOB and TEM). All these characteristics observed in tumors correspond to poorly differentiated carcinomas (possibly of the serous papillary type) [7]. The first-choice treatment for ovarian cancer (with anaplasia IV degree) is paclitaxel and carboplatin since both compounds exert their effects through different mechanisms of action [1]. Carboplatin can generate DNA adducts to prevent cell proliferation [8], and paclitaxel can bind to β-tubulin to stabilize the microtubules and block the mitosis, which triggers cell death by apoptosis [9]. Therefore, the similar effect that induced the RHTR compounds present in AE and AF02 to drugs used in chemotherapy for ovarian

cancer (particularly with carboplatin) makes them suitable candidates for more comprehensive structural studies and sheds light on their potential application against this disease.

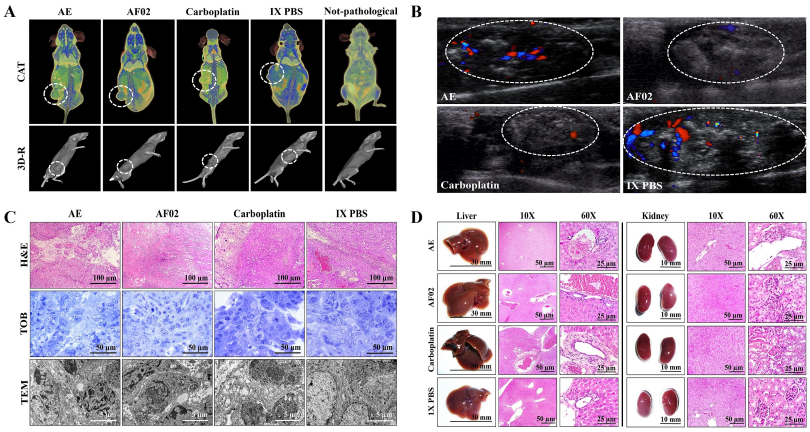

Figure 3. Imaging and histopathologic studies of ovarian tumor lesions and organs of *Nu/Nu* mice treated with RHTR. Analyses with CAT (**A**) and USG (**B**) were performed to observe densitometric and morphological changes in the tumoral lesions, as well as to rule out metastatic processes during the treatments. The tumor lesions are delimited with a white circle. In the Doppler color modality, the arterial and venous flow are indicated in red and blue, respectively. Differential histological patterns were observed in the tumor lesions (**C**) and the absence of tissue damage in the liver and kidneys (**D**) with treatment with AE and AF02 from RHTR at 200 mg/kg/i.p. for 28 days. Results show the mean ± SD of two biological replicates (n = 5). The positive control was carboplatin (50 mg/kg/i.p./3 alternating days per week in mice). RHTR, *Rhus trilobata*; AE, aqueous extract; AF02, aqueous fraction-02 (active fraction obtained with ethyl acetate); CAT, computer axial tomographic; 3D-R, 3D reconstruction; USG, ultrasonography; H&E, hematoxylin and eosin; TOB, toluidine blue; MET, transmission electron microscopy.

3.2. Morphometric and Paraclinical Studies of Mice Treated with RHTR

Anatomical lesions (**Figure 3**D) or morphometric changes (Table S1) in the liver and kidneys were absent in mice treated with RHTR. Additionally, histopathological lesions in the organs were not found by comparison with the control group (1× PBS; **Figure 3**D). Finally, paraclinical studies revealed slight leukopenia in mice treated with AE and AF02 at 28 days of administration concerning reference values for mice ($p \leq 0.05$, ANOVA; **Table 2**). The biochemical analysis demonstrated a decrease in albumin for mice treated with AE and AF02, whereas urea decreased with AE treatment at the end of the study ($p \leq 0.05$, ANOVA; **Table 2**). The results suggest slight hematopoiesis suppression in the bone marrow with AE and AF02 treatments, possibly by the quickly replicative phenotype of blood cells [10]. Additionally, paraclinical studies did not reveal hepatic dysfunction or renal failure, so the use of RHTR as an alternative treatment for ovarian cancer could be considered.

Table 2. Paraclinical studies in *Nu/Nu* mice treated with RHTR.

Treatments	AE	AF02	Carboplatin	1× PBS	Reference Range (mean)
Glucose (mg/dL)	72 ± 23.9	114 ± 21.2 *	107 ± 14.8 *	78.3 ± 16.6	63–176 (89)
Triglycerides (mg/dL)	71.5 ± 26.2	80 ± 11.35	103.7 ± 12.7 *	87.6 ± 12.01	55–115 (85)
Cholesterol (mg/dL)	66 ± 25.4 *	62 ± 2.52 *	108.6 ± 19.4 *	85.5 ± 13.4	26–82 (64)
Protein (g/dL)	4.48 ± 0.6	4.42 ± 0.62	5.1 ± 1.46	4.7 ± 0.56	4–8.6 (6.2)
Albumin (g/dL)	2.1 ± 0.8 *	2.03 ± 0.35 *	1.33 ± 0.29	1.36 ± 0.21	2.5–4 (3.2)
AST (GOT) (U/L)	132.6 ± 45.7	145.7 ± 7.69	162.9 ± 8.2	149.8 ± 27.29	55–251 (139)
ALT (GPT) (U/L)	41.2 ± 9.8	32.43 ± 19.2	64.4 ± 6.87 *	40.75 ± 14.5	17–77 (47)
Total bilirubin (mg/dL)	0.47 ± 0.07 *	0.39 ± 0.08 *	0.58 ± 0.2	0.67 ± 0.16	0.20–1.0 (0.6)
Alkaline phosphatase (U/L)	46.5 ± 23.2 *	83.6 ± 24.04	66.6 ± 15.6	71 ± 10.36	9–88 (48.5)
Creatinine (mg/dL)	0.74 ± 0.4	0.7 ± 0.25	0.37 ± 0.26 *	0.65 ± 0.2	0.2–0.9 (0.5)
Urea (mg/dL)	40.8 ± 8.2	57.6 ± 10.7	59.4 ± 9.99	47.9 ± 7.16	46.9–73 (60.1)

Treatments	AE	AF02	Carboplatin	1× PBS	Reference Range (mean)
BUN (g/dL)	19 ± 3.8	26.8 ± 4.7	27.8 ± 4.63	22.36 ± 3.32	11–27 (19)
Hemoglobin (g/dL)	15.2 ± 0.98	12.35 ± 2.2	13.1 ± 1.61	14.4 ± 2.13	10–17 (13.1)
Hematocrit (%)	48.3 ± 7.92	43.6 ± 17.8	40.57 ± 4.16	44.52 ± 2.17	39–49 (40.4)
Erythrocytes (×10^6/mm^3)	7.24 ± 1.06	7.67 ± 2.26	7.81 ± 0.88	7.92 ± 1.93	8.3
Leukocytes (×100/mm^3)	3600 ± 903 *	4242.6 ± 980	2750 ± 777 *	5720 ± 684	5–12 (6.33)
Platelets (×10^6/µL)	736 ± 1.414	689 ± 5.425	759 ± 19.143	710 ± 6.716	116
PCT	0.53 ± 0.07	0.49 ± 0.10	0.55 ± 0.29	0.55 ± 0.30	--

Results show the mean ± SD of two biological replicates (n = 5). *, $p \leq 0.05$ vs. control values treated with 1× PBS vehicle (ANOVA). The positive control was carboplatin (50 mg/kg/i.p./3 alternating days per week in mice). Reference range provided by the paraclinical laboratory (Merasoma Laboratory), minimum and maximum normal value for the analyte of interest in mice, and the respective midrange [11][12]. RHTR, *Rhus trilobata*; AE, aqueous extract; AF02, aqueous fraction-02 (active fraction); AST (GOT), aspartate aminotransferase; ALT (GPT), alanine aminotransferase; BUN: blood urea nitrogen; PCT: plateletcrit.

4. Purified Metabolites in RHTR

Methyl gallate (methyl 3,4,5-trihydroxybenzoate, $C_8H_8O_5$) was purified from RHTR and identified by nuclear magnetic resonance (NMR). The signal obtained was ^{1}H-NMR (300 MHz, CD_3OD) δ: 7.07 (H-2, H-6), δ: 4.9 (H-3, H-4, H-5), δ: 3.8 (H-8) (Figure S1A). ^{13}C-NMR (300 MHz, CD_3OD) δ: 122.3 (C-1), δ: 110.9 (C-2, C-6), δ: 147.3 (C-3, C-5), δ: 140.6 (C-) 4), δ: 169.8 (C-7), δ: 53.1 (C-8) (Figure S1B). The identification pattern obtained is similar to those reported by other authors [13][14]. Methyl gallate is present in several species of the *Rhus* genus [15] and exhibited antioxidant, antimicrobial, and antineoplastic activity in various investigations [16][17][18]; therefore, the biological activity of methyl gallate was evaluated in SKOV-3 cells.

5. Phytochemical Composition and in Silico Analysis of AF02-RHTR

The metabolite profile of AF02 showed a higher abundance of flavonoid and lipid compounds (**Table 3**). Additionally, a comparative study between the metabolite profile of AE and AF02 showed that epigallocatechin 3-cinnamate (3), 3,5-digalloylepicatechin (4), Myr (5), myricitrin (6), quercetin (9), hibiscoquinone A (11), quercitrin (12), myricetin 3-(4''-galloylrhamnoside) (13), obtusaquinol (14), epifisetinidol-(4$\beta\rightarrow$8)-catechin (15), 12*S*-hydroxy-16-heptadecynoic acid (18), (-)-pinellic acid (19), 11,14-eicosadienoic acid (20), amentoflavone (21), 3-(1,1-dimethylallyl)-8-(3,3-dimethylallyl)xanthyletin (22), lignocerate (23), and 2*R*-hydroxy-9*Z*,12*Z*-octadecadienoic acid (24) had a high relative abundance (double) in AF02 (**Table 3**, **Figure 4**A). These compounds were identified by their fragmentation patterns and the matching of their retention times with analytical standards (Figure S2). A comprehensive analysis of the fractions revealed that compound 5 (RT: 8.27 min) was present in all fractions and had higher relative abundance in AF02 (**Figure 4**A). Myr is a compound that was reported to have cytotoxic activity against different cancer cell lines [19]. Therefore, Myr could be related to the antineoplastic activity of RHTR on ovarian cancer studied in this project. To delimit the scope of this study, the experimental design focused on an in silico analysis and bibliographic search of the medicinal properties of the major metabolites in AF02-RHTR to determine its possible activity against ovarian cancer (**Table 3**). However, the choice of this design most likely generated a bias in which possibly, unintentionally, some active compounds in low concentration or the synergistic effect that can be generated by the combined presence of several compounds were omitted. This opens the possibility for future studies aimed at elucidating these two possibilities, either by our own group or by members of the community interested in studying natural compounds with potential anticancer bioactivity. Compounds that presented a higher score in the drug-likeness model were: 4 (DLMS: 1.52), 6 (DLMS: 0.78), 9 (DLMS: 0.93), 12 (DLMS: 1.04), 13 (DLMS: 1.12), 15 (DLMS: 0.61), and 21 (DLMS: 0.51) (**Table 3**). However, Myr presented a –0.04 value, possibly due to the low specificity of its pharmacological effect. These compounds are classified as flavonoids and were identified in other species of the *Rhus* genus, which mainly show antioxidant, anti-inflammatory, and cytotoxic activities (**Table 3**) [15]. Consequently, compounds 5 (RT: 8.27 min), 6 (RT: 8.47 min), 9 (RT: 8.60 min), 12 (RT: 9.45 min), and 16 (RT: 11.92 min) were selected to further evaluate their cytotoxic activity against SKOV-3 cells.

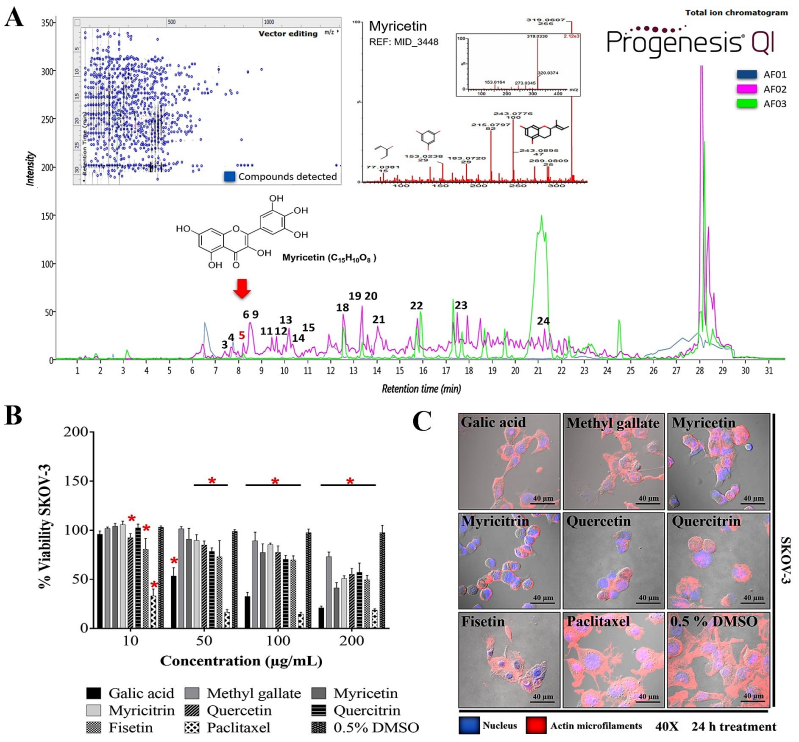

Figure 4. Metabolite profile of RHTR fractions and biological activity in cell lines. Total ion chromatograms (ESI+) for AF01, AF02, and AF03 revealed the presence of myricetin (RT: 8.27 min) in all of them (**A**). Compounds with higher relative abundance in AF02 are indicated (**A**). The vector map indicates 215 putative identifications of 555 compounds found in AF02 (**A**). Comparisons with the fragmentation pattern of myricetin in AF02 and an analytical standard (**A**). The IC_{50} of metabolites from RHTR was determined by dose-response viability curves with an MTT assay for 24 h in SKOV-3 cells (**B**), and morphological changes were determined by immunofluorescence with phalloidin-rhodamine (actin microfilaments) and DAPI (nucleus) in the same conditions (**C**). Results show the mean ± SD of three biological replicates (n = 3, in triplicates); * $p \leq 0.05$ vs. the vehicle group without treatment (0.5% DMSO) (ANOVA). RHTR, *Rhus trilobata*; AF, aqueous fraction (numbers indicate the fraction obtained after fractionation on solid-phase with solvents, as described in the Methodology).

Table 3. Major phytochemical compounds in AF02-RHTR by UPLC-MS^E.

No.	RT (min)	PI	Compound Name	Biological Activity	Presence in Plants	DLMS
1	6.18	HMDB41635	myricetin 3-arabinoside	Antioxidant, anticarcinogenic	*Rhus* spp.	0.90
2	6.44	CSID70398	methyl gallate *	Antioxidant	*Rhus* spp.	−0.49
3	7.05	HMDB38831	epigallocatechin 3-cinnamate	Antioxidant, antibacterial	*Ocotea porosa*	0.24
4	7.36	CSID3525015	3,5-digalloylepicatechin	Antioxidant	--	1.52
5	8.27	CHEBI:18152	myricetin *	Antioxidant, antineoplastic	*Rhus* spp.	−0.04
6	8.47	LMPK12112436	myricitrin *	Antioxidant, antineoplastic	*Rhus* spp.	0.78
7	8.52	LMPK12110568	quercetin 3-(2'''-galloylglucosyl)-(1→2)-alpha-L-arabinofuranoside	Antioxidant	*Euphorbia pachyrhiza*	1.24
8	8.52	CHEBI18082	1,2,3,4,6-pentakis-*O*-galloyl-*β*-D-glucose	Antineoplastic	*Rhus* spp.	0.35
9	8.60	CHEBI:16243	quercetin *	Antioxidant, anti-inflammatory, antineoplastic	*Rhus* spp.	0.93
10	9.13	CSID24784962	4-*O*-digalloyl-1,2,3,6-tetra-*O*-*β*-D-galloylglucose	Antibacterial, antineoplastic, antithrombotic	*Rhus typhina*	0.35

No.	RT (min)	PI	Compound Name	Biological Activity	Presence in Plants	DLMS
11	9.45	CHEBI:5715	hibiscoquinone a	Antioxidant	*Hibiscus* spp.	−0.52
12	9.45	LMPK12112171	quercitrin *	Antioxidant, antineoplastic	*Rhus* spp.	1.04
13	9.96	LMPK12112447	myricetin 3-(4''-galloylrhamnoside)	Antioxidant	--	1.12
14	10.20	LMPK12100067	obtusaquinol	Antiparasitic, nitric oxide inhibitor	*Dalbergia* spp.	−0.03
15	10.94	CSID35013429	epifisetinidol-(4*β*→8)-catechin	Antibacterial, *α*-amylase and lipase inhibitor	*Cotinus coggyria*	0.61
16	11.92	LMPK12111566	fisetin *	Antineoplastic, antioxidant, antiangiogenic	*Rhus* spp.	0.76
17	12.54	LMFA01010048	margaric acid	Antioxidant, antifungal	*Rhus typhina*	−0.33
18	12.54	LMFA01050146	12*S*-hydroxy-16-heptadecynoic acid	Anti-inflammatory	--	−0.38
19	13.37	CSID8034429	(-)-pinellic acid	Metabolism, adjuvant activity	*Pinelliae tuber*	−1.08
20	13.37	LMFA01030130	11,14-eicosadienoic acid	Antioxidant, anti-inflammatory	*Rhus typhina*	−0.08
21	13.9	LMPK12040009	amentoflavone	Antioxidant, anti-inflammatory	*Rhus* spp.	0.51
22	15.94	CSID10297786	3-(1,1-dimethylallyl)-8-(3,3-dimethylallyl) xanthyletin	--	*Ruta graveolens*	−1.31
23	17.7	CHEBI:31014	lignocerate	Anti-inflammatory	*Oleandra neriiformis*	−0.33
24	21.28	LMFA02000057	2*R*-hydroxy-9*Z*,12*Z*-octadecadienoic acid	Anti-allergic	*Brassica campestris*	−0.96

Results of three biological replicates (n = 3, in triplicates). Compounds putatively identified based on the fragmentation pattern and metabolic databases (AraCyc, PlantCyc, KEGG). DLMS: –6 to –1, non-drug compound / 0 to 2, drug-like compound. * Compounds confirmed with analytical standards. RHTR, *Rhus trilobata*; AF02, aqueous fraction-02 (active fraction); RT, retention time (min); PI, putative identity; DLMS, drug-likeness model score.

6. Biological Activity of Active Metabolites from RHTR in Cell Lines

The biological activity of purified compounds in RHTR such as Ga [6] and methyl gallate (2) was evaluated. Additionally, compounds selected from the in silico analysis, such as 5, 6, 9, 12, and 16, were evaluated in cancer and normal epithelial cells. The results showed that the compounds had biological activity in SKOV-3 (**Figure 4**B) and OVCAR-3 (Figure S3A) cell lines at concentrations lower than 200 µg/mL (**Table 4**). However, Ga (50/43 µg/mL) and Myr (166/94 µg/mL) had the highest activity compared with the vehicle group (0.5% DMSO) ($p \leq 0.05$, Dunnett). The biological activity of both compounds was corroborated in CACO-2 cells (Figure S3B) at 25 and 62 µg/mL, respectively ($p \leq 0.05$, Tukey; **Table 4**). Similarly, both compounds presented cytotoxic activity in CHO-K1 and BEAS-2B cells (Figure S3C,D) at ~150 µg/mL, possibly through a genotoxic effect related to reactive oxygen species (ROS) production [20][21]. The highest activity was observed with Myr at 33 µg/mL in CHO-K1 and Ga at 25 µg/mL in BEAS-2B; the lowest activity was found with quercitrin and methyl gallate at 200 µg/mL in both cell lines ($p \leq 0.05$, Dunnett) (**Table 4**). These results demonstrated that the biological activity of the compounds considerably depends on the cellular phenotype. Cell morphology analysis in SKOV-3 revealed that the compounds induced cellular changes such as individualization, rounding, microfilaments loss, cytoplasm condensation, nuclear fragmentation, and cell monolayer breakdown after 24 h of treatment, and these effects were similar to those for the paclitaxel group (**Figure 4**C). Cells treated with vehicle (0.5% DMSO) presented lamellipodia, filopodia, stress fibers, adhesion dots, mitosis, confluence, and cell monolayer formation (**Figure 4**C).

Table 4. Biological and cytotoxic activity of metabolites from RHTR in cell lines.

Sample/Cell Line	SKOV-3	OVCAR-3	CACO-2	BEAS-2B	CHO-K1
Gallic acid	**50 (294)**	**43 (253)**	**25 (147)**	**25 (147)**	**100 (588)**
Methyl gallate	**>200 (1,086)**	**>200 (1,086)**	**100 (543)**	**200 (1,086)**	**130 (706)**
Myricetin	**166 (522)**	**94 (295)**	**62 (195)**	**64 (201)**	**33 (104)**
Myricitrin	**197 (424)**	**200 (431)**	**>200 (431)**	**160 (344)**	**94 (202)**
Quercetin	**>200 (662)**	**200 (662)**	**150 (496)**	**189 (625)**	**127 (420)**
Quercitrin	**>200 (446)**	**>200 (446)**	**179 (399)**	**>200 (446)**	**>200 (446)**
Fisetin	**200 (699)**	**200 (699)**	**100 (349)**	**50 (175)**	**46 (161)**
Paclitaxel	**7 (8.20)**	**8 (9.37)**	**20 (23.42)**	**8 (9.37)**	**10 (11.71)**

Results show the half-maximal inhibitory concentration (IC_{50}, µg/mL and [µM]) obtained of three biological replicates (n = 3, in triplicates). The positive control was paclitaxel.

The results showed that the principal metabolites in RHTR against ovarian cancer cells could be Ga and Myr. These compounds are active in multiple cancer cell lines through ROS generation (amongst other processes) that triggers cell death by apoptosis [19][22]. Complementary studies by our research group in mouse models for ovarian cancer demonstrated that Ga and Myr at 50 mg/kg administered by the peritumoral route inhibited tumoral lesions (50% of progression), decreased vascularity, and induced apoptosis, with few toxicological effects, possibly by a mechanism related to carbonic anhydrase-IX or PI3K [23]. However, there is the possibility that other metabolites in RHTR (majority or present) could have specific activity against different cancer types because cancer cells can develop a sensitivity or selective resistance to certain drugs classes related to the phenotypic and functional heterogeneity, as well as molecular features present in each neoplasm disease [24]. Therefore, these findings could be a perspective to address in future studies. Similarly, additional studies are required to demonstrate if the antineoplastic activity observed in RHTR results from a synergistic mechanism among other abundant compounds in the plant such as β-PGG (**Table 3**) [25][26]. Recent studies have demonstrated that β-PGG can induce cell cycle arrest in breast cancer (MCF-7, 50 µM) in the G_1 phase by inhibiting kinase activity in the D/CDK4 and CDK2 complex, decreasing the phosphorylation in retinoblastoma protein (pRB), and increasing the levels of p27Kip, p21Cip, and p53 [27][28]. Thus, β-PGG could be involved in the biological activity found in RHTR; however, more in-depth studies are required to confirm this claim. Finally, the results show that RHTR, Ga, and Myr could play a role in the alternative treatment of ovarian cancer.

References

1. Gallardo-Rincón, D.; Espinosa-Romero, R.; Muñoz, W.R.; Mendoza-Martínez, R.; Villar-Álvarez, S.D.; Oñate-Ocaña, L.; Isla-Ortiz, D.; Márquez-Manríquez, J.P.; Apodaca-Cruz, Á.; Meneses-García, A. Epidemiological overview, advances in diagnosis, prevention, treatment and management of epithelial ovarian cancer in Mexico. Salud Publica Mex. 2016, 58, 302–308.
2. DeFriend, D. Ovarios. In Ultrasonido Clinico; Allan, P., Baxter, G., Weston, M., Eds.; Amolca: Ciudad de México, Mexico, 2016; pp. 660–685. ISBN 9789588760827.
3. Posada-Torres, J.A.; Del Real-Ordóñez, S.; Salcedo-Hernández, R.A. Capítulo 8, Tratamiento quirúrgico inicial: ¿rutina en ovario?, ¿existen variaciones en la cirugía para enfermedad temprana y avanzada. In COI: Cáncer de Ovario Epitelial; Gallardo-Rincón, D., Meneses-García, A., De la Garza-Salazar, J.G., Juárez-Sanchez, P., Aguilar-Ponce, J.L., Eds.; PyDESA: Ciudad de México, Mexico, 2016; pp. 87–93.
4. Varela-Rodríguez, L.; Sánchez-Ramírez, B.; Rodríguez-Reyna, I.S.; Ordaz-Ortiz, J.J.; Chávez-Flores, D.; Salas-Muñoz, E.; Osorio-Trujillo, J.C.; Ramos-Martínez, E.; Talamás-Rohana, P. Biological and toxicological evaluation of Rhus trilobata Nutt. (Anacardiaceae) used traditionally in Mexico against cancer. BMC Complementary Med. Ther. 2019, 19, 1–18.
5. Abbott, B.J.; Leiter, J.; Hartwell, J.L.; Caldwell, M.E.; Beal, J.L.; Perdue, R.E.; Schepartz, S.A. Screening data from the cancer chemotherapy national service center screening laboratories. XXXIV. Plant extracts. Cancer Res. 1966, 26, 1131–1271.
6. Pettit, G.R.; Saldana, E.I.; Lehto, E. Antineoplastic agents 35. Rhus trilobata. Lloydia 1974, 37, 539–540.
7. National Comprehensive Cancer Network (NCCN). Guidelines V. 1.2016: Ovarian Cancer. 2016. Available online: https://jnccn.org/view/journals/jnccn/14/9/articlep1134.xml#container-4698-item-4697 (accessed on 7 July 2021).

8. Micetick, K.C.; Barnes, D.; Erickson, L.C. A comparative study of the cytotoxicity and DNA-damaging effects of cis-(dimamino) (1,1-cyclobutanedicarboxylato)-platinum (II) and cis-diamminedichloroplatinum (II) on L1210 cells. Cancer Res. 1985, 45, 4043–4047.
9. Zhu, L.; Chen, L. Progress in research on paclitaxel and tumor immunotherapy. Cell. Mol. Biol. Lett. 2019, 24, 1–11.
10. Adeneye, A.A.; Ajagbonna, O.P.; Adeleke, T.I.; Bello, S.O. Preliminary toxicity and phytochemical studies of the stem bark aqueous extract of Musangacecropioides in rats. J. Ethnopharmacol. 2006, 105, 374–379.
11. Fernandes, D.P.; Pimentel, M.M.; Dos Santos, F.A.; Praxedes, E.A.; De Brito, P.D.; Lima, M.A.; Lelis, I.C.N.; De Macedo, M.F.; Bezerra, M.B. Hematological and biochemical profile of BALB/c nude and C57BL/6 SCID female mice after ovarian xenograft. An. Da Acad. Bras. De Ciências 2018, 90, 3941–3948.
12. Otto, G.P.; Rathkolb, B.; Oestereicher, M.A.; Lengger, C.J.; Moerth, C.; Micklich, K.; Fuchs, H.; Gailus-Durner, V.; Wolf, E.; Hrabě de Angelis, M. Clinical chemistry reference intervals for C57BL/6J, C57BL/6N, and C3HeB/FeJ mice (Mus musculus). J. Am. Assoc. Lab. Anim. Sci. 2016, 55, 375–386.
13. Kamatham, S.; Kumar, N.; Gudipalli, P. Isolation and characterization of gallic acid and methyl gallate from the seed coats of Givotia rottleriformis Griff. and their anti-proliferative effect on human epidermoid carcinoma A431 cells. Toxicol. Rep. 2015, 14, 520–529.
14. Mohd Nazrul Hisham, D.; Mohd Lip, J.; Mohd Noh, J.; Normah, A.; Nurul Nabilah, M.F. Identification and isolation of methyl gallate as a polar chemical marker for Labisia pumila Benth. J. Trop. Agric. Food Sci. 2011, 39, 279–284.
15. Rayne, S.; Mazza, G. Biological activities of extracts from Sumac (Rhus spp.): A review. Plant Foods Hum. Nutr. 2007, 62, 165–175.
16. Kim, H.; Lee, G.; Sohn, S.-H.; Lee, C.; Kwak, J.W.; Bae, H. Immunotherapy with methyl gallate, an inhibitor of Treg cell migration, enhances the anti-cancer effect of cisplatin therapy. Korean J. Physiol. Pharmacol. 2016, 20, 261–268.
17. Khurana, S.; Hollingsworth, A.; Piche, M.; Venkataraman, K.; Kumar, A.; Ross, G.M.; Tai, T.C. Antiapoptotic Actions of Methyl Gallate on Neonatal Rat Cardiac Myocytes Exposed to H2O2. Oxidative Med. Cell. Longev. 2014, 2014, 1–9.
18. Lee, H.; Lee, H.; Kwon, Y.; Lee, J.-H.; Kim, J.; Shin, M.-K.; Kim, S.-H.; Bae, H. Methyl gallate exhibits potent antitumor activities by inhibiting tumor infiltration of CD4+ CD25+ regulatory T cells. J. Immunol. 2010, 185, 6698–6705.
19. Devi, K.P.; Rajavel, T.; Habtemariam, S.; Nabavi, S.F.; Nabavi, S.M. Molecular mechanisms underlying anticancer effects of myricetin. Life Sci. 2015, 142, 19–25.
20. Hobbs, C.A.; Swartz, C.; Maronpot, R.; Davis, J.; Recio, L.; Koyanagi, M.; Hayashi, S.-M. Genotoxicity evaluation of the flavonoid, myricitrin, and its aglycone, myricetin. Food Chem. Toxicol. 2015, 83, 283–292.
21. Marcarini, J.C.; Ferreira-Tsuboy, M.S.; Cabral-Luiz, R.; Ribeiro, L.R.; Hoffmann-Campo, C.B.; Ségio-Mantovani, M. Investigation of cytotoxic, apoptosis-inducing, genotoxic and protective effects of the flavonoid rutin in HTC hepatic cells. Exp. Toxicol. Pathol. 2011, 63, 459–465.
22. Badhani, B.; Sharma, N.; Kakkar, R. Gallic acid: A versatile antioxidant with promising therapeutic and industrial applications. RSC Adv. 2015, 5, 27540–27557.
23. Varela-Rodríguez, L.; Sánchez-Ramírez, B.; Hernández-Ramírez, V.I.; Varela-Rodríguez, H.; Castellanos-Mijangos, R.D.; González-Horta, C.; Chávez-Munguía, B.; Talamás-Rohana, P. Effect of Gallic acid and Myricetin on ovarian cancer models: A possible alternative antitumoral treatment. BMC Complementary Med. Ther. 2020, 20, 1–16.
24. Zhu, X.; Li, S.; Xu, B.; Luo, H. Cancer evolution: A means by which tumors evade treatment. Biomed. Pharmacother. 2021, 133, 1–13.
25. Shin, H.; Park, Y.; Choi, J.H.; Jeon, Y.H.; Byun, Y.; Sung, S.H.; Lee, K.Y. Structure elucidation of a new triterpene from Rhus trichocarpa roots. Magn. Reson. Chem. 2017, 55, 763–766.
26. Gross, G.G. Enzymes in the Biosynthesis of Hydrolyzable Tannins. In Plant Polyphenols: Synthesis, Properties, Significance; Hemingway, R.W., Laks, P.E., Branham, S.J., Eds.; Springer: New York, NY, USA, 1992; pp. 43–60.
27. Chen, W.J.; Chang, C.Y.; Lin, J.K. Induction of G1 phase arrest in MCF human breast cancer cells by pentagalloylglucose through the down-regulation of CDK4 and CDK2 activities and up-regulation of the CDK inhibitors p27(Kip) and p21(Cip). Biochem. Pharmacol. 2003, 65, 1777–1785.
28. Hu, H.; Lee, H.J.; Jiang, C.; Zhang, J.; Wang, L.; Zhao, Y.; Xiang, Q.; Lee, E.O.; Kim, S.H.; Lü, J. Penta-1,2,3,4,6-O-galloyl-β-D-glucose induces p53 and inhibits STAT3 in prostate cancer cells in vitro and suppresses prostate xenograft tumor growth in vivo. Mol. Cancer Ther. 2008, 7, 2681–2691.